RSC Advances

ROYAL SOCIETY OF CHEMISTRY

www.rsc.org/advances

Fe^{3+}-induced oxidation and coordination cross-linking in catechol-chitosan hydrogels under acidic pH conditions

Zhongwei Guo, Kefeng Ni, Dongzhi Wei, Yuhong Ren*

State Key Laboratory of Bioreactor Engineering, East China University of Science and Technology, Shanghai 200237, China.

KEYWORDS: biomimetic materials, catecholate polymer, dual crosslinking system, hydrogel

ABSTRACT

Mussel byssus is rich in Fe^{3+} and catechol-containing proteins; chemical interactions between these components vary widely with respect to changes in pH during byssal maturation. Previous studies have indicated the key role played by Fe^{3+}-catechol interactions in regulating many attributes of biological materials, such as toughness, extensibility, and self-assembly. In this study, a platform based on a highly substituted catechol-modified chitosan (70%, CCS) was used to investigate the effect of pH on the reactions between Fe^{3+} and catechols. This study demonstrated that the Fe^{3+}-induced CCS hydrogel is essentially a dual cross-linking system composed of covalent and

coordination crosslinks, under acidic pH conditions. Variations in the Fe^{3+}-catechol molar ratios could strongly affect the gelation time, physical properties, and UV-vis and Raman spectra. These changes represented different balance state between oxidation and coordination mechanism in the hydrogel network. In addition, the system was subjected to optical microscopy and SEM in order to obtain a visual description of the dual-crosslinking mechanism.

1. Introduction

Mussel byssal threads are strong, resilient shock-absorbing biological materials composed of two distinct regions: a fibrous inner core and an outer cuticle. Previous research has revealed that the cuticle is rich in catechol-containing proteins and inorganic ions, especially Fe^{3+}.[1-4] The complex mechano-chemical interactions between Fe^{3+} and the catechols endow the cuticle with excellent mechanical performance, characterized by high hardness and extensibility, and self-healing properties. In addition, the cuticles demonstrate remarkable mechanical properties, which have been hypothesized to originate from both organic (covalent) and inorganic (metal coordination) bonds.[1,5–8] Growing evidence points towards the considerable impact exerted by metal-biomolecule interactions on the properties of these materials.[9–12] Although the mechanism of interaction between the metal and biomolecules could serve as a valuable reference to improve the mechanical properties of synthetic materials, these are yet to be substantially elucidated.

Several researchers have attempted the fabrication of synthetic materials inspired by mussel byssal threads, in order to elucidate the Fe^{3+}-catechol interaction mechanisms.[13,14] The coordination between Fe^{3+} and catechols is strongly dependent on the pH, and Fe^{3+} does not effect a significant covalent cross-linking via oxidation of catechols, in a pH-controlled catechol-Fe^{3+} cross-linking polymer.[15] However, spectroscopic evidence has linked the presence of Fe^{3+} to catechol oxidation for decades.[8,16,17] It has been reported that catechol-modified polyethylene glycol (PEG) polymers could be covalently cross-linked under acidic pH conditions in the presence of Fe^{3+}.[18,19] In addition, Fe^{3+}-catechol gels equilibrated at pH 3 fit the description of Hookean elastic materials at low strains because of their purely covalent nature, with no coordination crosslinking formed under such acidic pH conditions.[18–20] Therefore, the mechanism of interactions between Fe^{3+} and catechols must be extensively investigated.

Chitosan (CS), a natural, linear amino polysaccharide obtained by partial deacetylation of chitin, is considered to be a promising material in the pharmaceutical, chemical, and food industry because of its special chemical (reactive -OH and $-NH_2$ groups) and biological (non-toxic, biodegradable, biocompatible) properties.[21,22] In this study, we have synthesized a catechol-functionalized chitosan (CCS, with a high degree of substitution) inspired by mussel byssal threads in order to investigate the complex interactions between Fe^{3+} and catechols at acidic pH. The gelation time, rheological properties, the results of UV-vis and Raman spectroscopy, and the morphological

characteristics were elucidated in order to characterize the crosslinking mechanism and the physical properties of the hydrogel systems.

2. Experimental section

2.1 Materials and reagents

Dopamine hydrochloride, chitosan (viscosity: 100-200mpa.s, deacetylation degree~ 95%), 3,4-dihydroxy benzaldehyde, sodium cyanoborohydride ($NaBH_3CN$), ethylene diamine tetraacetic acid (EDTA) disodium salt dehydrate, ferric chloride hexahydrate, and sodium periodate ($NaIO_4$) were purchased from Sigma-Aldrich (St. Louis, MO, USA). Other analytical grade chemicals were purchased from Sinopharm Chemical Reagent Co., Ltd. (Shanghai, China). All chemicals were used without further purification. Ultrapure water was obtained using a NANOpure Infinity® system (Barnstead-Thermolyne; Sigma-Aldrich). The degree of substitution of CS was calculated using ^{1}H-nuclear magnetic resonance (^{1}H-NMR, Bruker, Germany: AVANCE III 400).

2.2 Synthesis of catechol-modified chitosan (CCS)

CCS was synthesized by Bosch reduction of Schiff base, according to a previously reported method with modifications (Fig. 1a).[21] Briefly, 0.1 g CS powder was dissolved in 20 mL 1% acetic acid solution. Five milliliter DMF, containing 0.3 g 3,4-dihydroxy benzaldehyde was added to this solution, and incubated at room temperature for 6.5 h. Ten milliliter H_2O containing 0.3 g $NaBH_3CN$ was added to this mixture and incubated at

room temperature for another 6.5 h. The product was precipitated by addition of 300 mL ethanol, washed several times with H_2O and ethanol, dried in vacuum at room temperature for 3 hours, and stored under nitrogen at -20°C. ^{1}H-NMR of CCS was detected using the Bruker Avance III 400 ^{1}H-NMR spectrophotometer, using D_2O containing 1% DCl as the solvent (Fig. 1b). The calculation formula used was as follows:

$$\text{Substitution rate} = \frac{\frac{1}{3} \times \text{Signal intensity due to aromatic protons}}{\text{Signal intensity due to C-2 proton}} \times 100\%$$

2.3 Fe^{3+}-induced hydrogel formation

The CCS obtained as described in the previous section was used for all gel experiments. Stock solutions of $FeCl_3$ (148 mM, 296 mM, 445 mM) and CCS (catechol concentration: 58 mM, 38 mM, 19 mM) were prepared in 5% acetic acid (v/v). A typical procedure for gel formation included the mixing of 500 μL of the appropriate CCS solution with 65 μL of the corresponding $FeCl_3$ stock solution. Specifically, Fe^{3+}-catechol ratios of 1:1, 1:2, and 1:3 were obtained by the addition of 65 μL of 148 mM $FeCl_3$ solution into 500 μL of 19, 38, and 58 mM CCS, respectively. In order to initiate gelation in the solution with Fe^{3+}-catechol ratios of 1:3, 2:3, and 3:3, 500 μL of the 58 mM CCS stock solution was mixed with 65 μL of the 148mM, 296mM, and 445mM of $FeCl_3$ stock solutions, respectively. This caused gelation and color development in the solutions, according to the Fe^{3+}-catechol ratios. The gel was physically mixed until a homogenous color and physical state was established. The gelation time was calculated by the

inversion method.

2.4 IO_4^--induced hydrogels

The protocol described in the previous section for the preparation of Fe^{3+}-induced hydrogels was followed for the preparation of IO_4^--induced hydrogels, substituting $FeCl_3$ with $NaIO_4$.

2.5 Rheology of Gels

The mechanical properties of the hydrogels were tested using a rheometer (ARES; TA Instruments, Newcastle, DE, USA) with parallel plate geometry (25 mm diameter rotating top plate) at 23°C. All tests were performed immediately after transferring the gel sample onto the sample stage. The gels were tested for oscillatory shear (as a function of frequency) at 10% strain from 30 rad/s to 0.1 rad/s, while measuring the storage modulus (G') and loss modulus (G''). Time tests were performed at 10% strain and 10 rad/s. The sample dehydration during testing was negligible, as the typical test time was less than 15 minutes. Data points represented the average of tests performed on three separate gels.

2.6 UV-vis spectroscopy

Fe^{3+}-induced catechol oxidation and coordination were monitored on a Hitachi U-5100 UV-vis spectrophotometer (Hitachi, Tokyo, Japan) using a quartz cuvette with a path length of 1 cm. All samples were initially blanked against 5% acetic acid. Solutions composed of different molar ratios of Fe^{3+} and catechol were obtained by mixing 50 μL

stock solutions of CCS with 6.5 µL of the corresponding stock solutions of $FeCl_3$ in 2 mL 5% acetic acid. The final solutions were thoroughly mixed before the final testing. Spectral changes in the 5% acetic acid solutions of 50 µL CCS (58 mM catechol) and 6.5 µL 148 mM $FeCl_3$ (Fe^{3+}-catechol ratio of 1:3) were observed upon increasing the pH using 1M NaOH.

2.7 Resonance Raman Spectroscopy

Resonance spectra were acquired using a Renishaw Raman InVia reflex microscope (Wotton-under-Edge, UK) equipped with an air-cooled charge-coupled device (CCD) camera. A Leica DMLM (Leica, Solms, Germany) camera, equipped with three objectives and a trinocular viewer that accommodated a video camera (allowing direct viewing of the sample), was attached to the spectrophotometer. The samples were excited at 514 nm with an argon ion laser (Modu-Laser LLC, Centerville, UT, USA). Laser power at a range of 10–30 mW was used for all measurements. The average of three spectra collected from different regions was taken for each sample. To facilitate clearer observation of the resonance peaks, the fluorescence background was subtracted.

2.8 Morphology of the hydrogels

The morphology of the hydrogels was observed through an optical microscope (DM2500; Leica), and the appropriate pictures taken using the attached digital camera. In order to elucidate the interior network morphology of the hydrogels, the freeze-dried

hydrogels were observed using a JEOL JSM-6360 LV scanning electron microscope (JEOL, Peabody, MA, USA). All specimens were coated with a conductive layer of sputtered gold. All experiments were performed at 25°C.

3. Results and discussion

3.1 Synthesis and characterization of the catechol-modified chitosan (CCS)

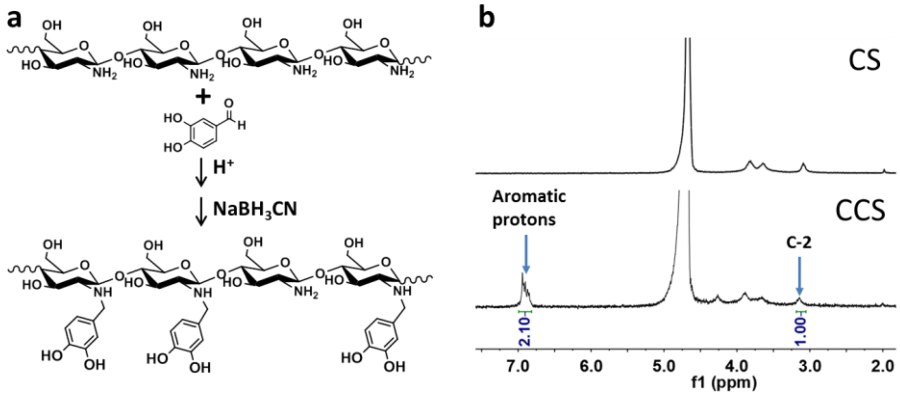

Fig. 1 (a) Synthetic reaction of catechol-chitosan (CCS) and (b) ^{1}H-NMR spectra of CS, CCS.

CCS, a catechol-containing linear polymer, was used in subsequent gel formation studies. Fig. 1a illustrated the synthesis route of CCS. CCS was synthesized by Bosch reduction of a Schiff base, obtained as a result of the reaction between chitosan (CS) and 3,4-dihydroxy benzaldehyde. The degree of substitution of CS was calculated based on the ^{1}H-NMR spectrum (Fig. 1b) of CCS. Under these reaction conditions, the degree of substitution was determined to be 70%.

3.2 Hydrogel formation

The CCS (obtained as described in the Experimental procedures) was used for all gel experimentation. All gels were prepared by mixing Fe^{3+} or IO_4^- with CCS in a 5% acetic acid solution (pH ~ 3) until a homogenous color and physical state were established. As seen in Fig. 2a, different molar ratios of Fe^{3+}-catechol resulted in changes in the color, as well as physical changes, from a green fluid to a purple/black gel. A covalently cross-linked polymer hydrogel was prepared via the $NaIO_4$-induced oxidation of CCS (Fig. 2b) for comparison.

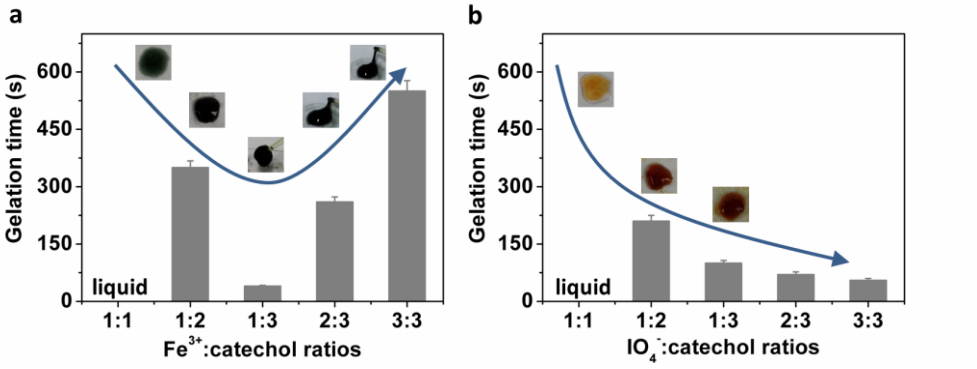

Fig. 2 Physical properties and gelation time of (a) Fe^{3+}-CCS hydrogels and (b) IO_4^--CCS hydrogels.

The impact of the molar quantities of catechols on the formation of Fe^{3+}-CCS hydrogels was investigated. Solutions containing Fe^{3+} and catechol at a ratio of 1:1 (Fe^{3+}, catechol: 17mM) did not form any gels, possibly because of insufficient crosslinking. When the molar quantities of catechols increased, i.e., when the Fe^{3+}-catechol ratio was increased from 1:2 to 1:3 in the solution, the gelation time decreased from 350 s to 40 s. This was also observed in the gelation time of IO_4^--induced CCS hydrogels (IO_4^--catechol ratio of 1:2, 210 s; 1:3, 100 s). These results suggest that the amount of crosslinking

formed in the system was directly proportional to the number of catechols included in the system, because of the proximity to Fe^{3+} or IO_4^-, which facilitates the chemical interactions such as oxidation and coordination.

Subsequently, we studied the influence of the molar quantities of Fe^{3+} on the formation of Fe^{3+}-CCS hydrogels. Generally, the presentation of greater molar quantities of Fe^{3+} would facilitate greater oxidation crosslinking under acidic pH conditions, thereby increasing the gelation rate.[18] However, as seen in Fig. 2a, the gelation time was increased from 40 s to 550 s when the Fe^{3+}-catechol stoichiometry ratio was increased from 1:3 to 3:3 (Fe^{3+}, catechol: 51mM). This change is contrary to the gelation time of IO_4^--induced gels (the gelation time at an IO_4^--catechol ratio of 1:3 was 100 s; 3:3 was 55 s, Fig. 2b). These results suggest that the Fe^{3+}-induced CCS hydrogel was not an oxidation-dominated system under acidic pH conditions; it could probably be a dual system including both coordination and oxidation crosslinking. The presentation of equimolar quantities of Fe^{3+} in the system led to the formation of mono-catecholate species (from catechols), thereby preventing coordination-based crosslinking that must proceed via bis- and tris-catecholate motifs. The substantial increase in gelation time also suggested that the Fe^{3+}-induced coordination crosslinking was more rapid compared to the oxidation crosslinking induced by its redox activity.

3.3 Hydrogel characterization

In order to elucidate the impact of the stoichiometry of the Fe^{3+}-catechol ratio on the mechanical properties of the hydrogels, the prepared hydrogels were tested using a rheometer. The $NaIO_4$-induced covalent crosslinking CCS hydrogels at IO_4^--catechol ratios of 1:2 and 1:3 were compared (Fig. 3a). These gels exhibited typical features of elastic solids; G′ and G′′ displayed natural frequency-independent behavior and G′ >>G′′. These results were similar to those obtained for other catechol-modified polymer hydrogels formed by $NaIO_4$-induced covalent crosslinking, which exhibited Hookean elastic properties under low strains.[14,18,20]

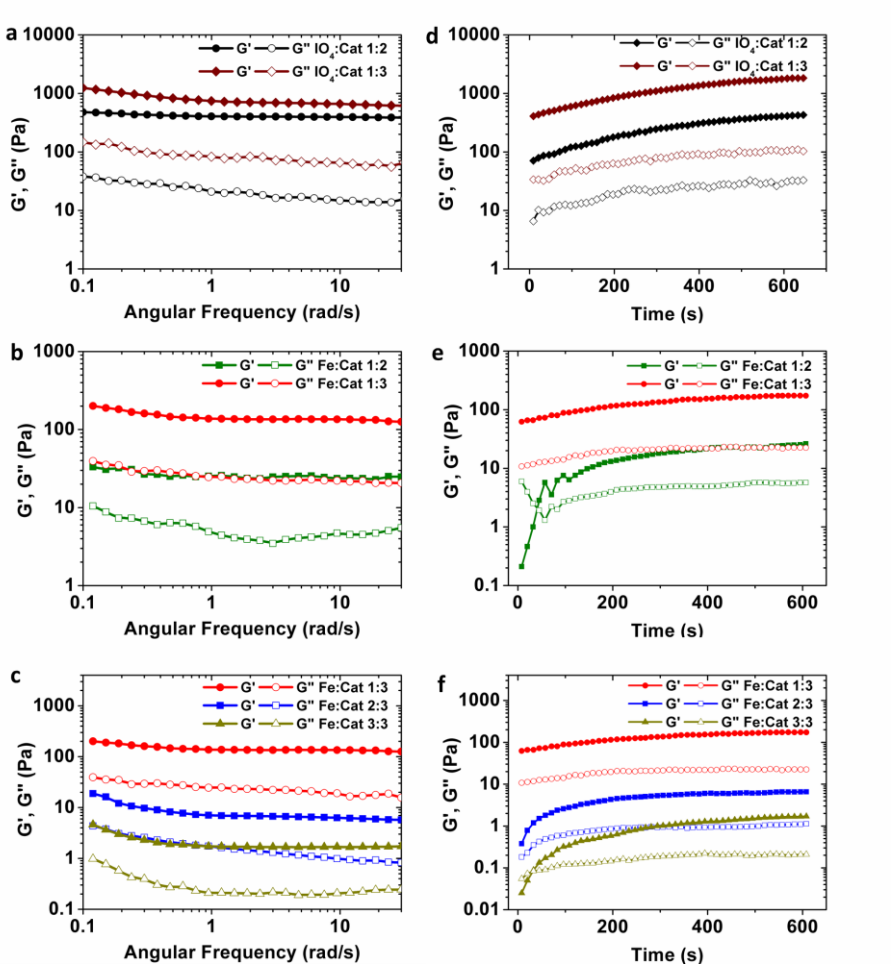

Fig. 3 Rheological properties of IO_4^--CCS hydrogels and Fe^{3+}-CCS hydrogels at pH~3. Gel formation was studied as a function of frequency (left) and time (right).

The frequency sweep of Fe^{3+}-induced CCS hydrogels (Fe^{3+}-catechol molar ratio of 1:2 and 1:3) are displayed in Fig. 3b. The modulus of hydrogels formed at an Fe^{3+}-catechol ratio of 1:3 was higher than that of gels formed at a ratio of 1:2, which was consistent with the higher crosslinking density. These results suggested that catechols bind Fe^{3+} in a bis-/tris-coordination type under insufficient Fe^{3+} conditions in the system, thereby increasing the degree of crosslinking. Fig. 3c demonstrates the frequency sweep of Fe^{3+}-induced CCS hydrogels (Fe^{3+}-catechol molar ratios of 1:3, 2:3, and 3:3). The gels were observed to become softer when greater quantities of Fe^{3+} were present in the system. This change could be a result of increased mono-Fe^{3+}-catechol species formation, preventing the occurrence of coordination-based crosslinking (that occurs via the bis-/tris-coordination type). These results support our interpretation of the gelation time data. Specifically, all Fe^{3+}-induced CCS hydrogels exhibited very special material properties. Neither hydrogels fit the descriptions of Hookean elastic or Maxwell viscoelasticity models.[15,18,20] These results suggested that the covalent and coordination crosslinking mechanisms were not especially dominant in the formation of Fe^{3+}-induced CCS hydrogels under acidic pH (pH ~ 3) conditions. And due to the dual cross-linking system, the rheological property of the Fe^{3+}-induced CCS hydrogel was worse than the one induced by IO_4^-. The presence of mechanically functional Fe^{3+}-catechol coordination

bonds endowed the hydrogels with new viscoelastic behavior that dissipate energy under applied force. In mussel byssus, these coordination bonds play an important role in transferring and mitigating loads between soft and hard tissues.[1,18]

Oscillatory time sweeps were performed to monitor the gelation process of IO_4^--CCS hydrogels and Fe^{3+}-CCS hydrogels. Fig. 3d demonstrates the time sweep profiles of G′ and G′′ for the IO_4^--CCS hydrogels. Although initial time points indicated elastic properties (G′ > G′′), qualitative observations by inversion method showed gelation time around 210 s and 100 s (IO_4^--catechol ratio of 1:2, 1:3). Within 300 s, the storage modulus of the hydrogels appeared to plateau (G′ and G′′ values at an IO_4^--catechol ratio of 1:2 was 300 Pa, 20 Pa; 1:3 was 900 Pa, 80 Pa). This indicated that the hydrogel's structure has reached an equilibrium state. As seen in Fig. 3e, solutions containing Fe^{3+} and catechol at a ratio of 1:2 were tested. Initially, G′′ was higher than G′, which was expected since the mixtures were still in liquid state. As the solutions began to gel and a cross-linked network was formed, the storage modulus began to increase and the elastic properties of the hydrogel began to dominate. Consequently, there was a crossover point where G′ became larger than G′′. With the increasing of time, the hydrogel's mechanical properties constantly increased until a steady value was obtained near 350 s (G′: 20 Pa, G′′: 4 Pa). However, when the Fe^{3+}-catechol ratio was increased from 1:2 to 1:3 in the solution, the gels formed rapidly and the crossover point of G′ and G′′ was not observed. Then the mixtures formed a stabilized gel at G′: 150 Pa and G′′: 23 Pa. Furthermore, with

increased Fe^{3+} concentration the crossover point appeared again (Fig. 3f), indicating that the cross-linking rate was decreased. And the gels were observed to become softer when greater quantities of Fe^{3+} were present in the system (G′ and G′′ values at an Fe^{3+}-catechol ratio of 1:3 was 150 Pa, 23 Pa; 2:3 was 6 Pa, 1 Pa; 3:3 was 2 Pa, 0.25 Pa).

A concentrated EDTA solution was used to study the stabilities of Fe^{3+}-induced CCS hydrogels, in order to further elucidate the balance of covalent and coordination crosslinking in these hydrogels (Fig. 4). Compared to other catechol-modified hydrogels induced by $NaIO_4$, no difference was observed in the constructed $NaIO_4$-induced CCS hydrogels upon exposure to the EDTA solution; this was because the covalent gels were stable in EDTA.[15,18]

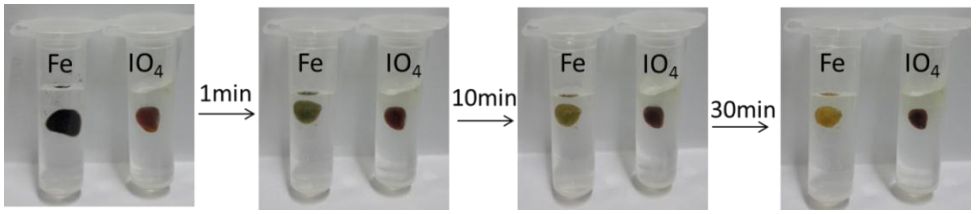

Fig. 4 EDTA treatment of Fe^{3+}- and IO_4^--gels. A small piece of each gel was immersed in 150 mM EDTA in 1% acetic acid (pH 3.7).

However, the gels formed at a Fe^{3+}-catechol ratio of 1:3 displayed significant changes in the color and physical properties. The dark gel with a smooth surface was converted to a pale yellow material with a rough and porous structure. This morphological change describes the disintegration of the coordination crosslinking network. Unlike the other coordination-dominated gel developed by Holten-Anderson et al,[15] this gel did not

dissolve in the EDTA solution. When this Fe^{3+}-gel was exposed to EDTA, the coordination crosslinking system was disrupted; because of its dual crosslinking mechanism, the covalently-crosslinked residues remained untouched.

3.4 UV-vis spectroscopy

The results of the UV-vis absorbance spectroscopy further demonstrated that Fe^{3+} induced both oxidative and coordinative behaviors in catechol under acidic pH conditions. Fig. 5a displays the UV-vis spectra of the IO_4^- and CCS mixture in 5% acetic acid. The addition of $NaIO_4$ resulted in an immediate color change in the solution from colorless to yellow, the signature color of *o*-quinone (λmax = 400 nm).[15–17]

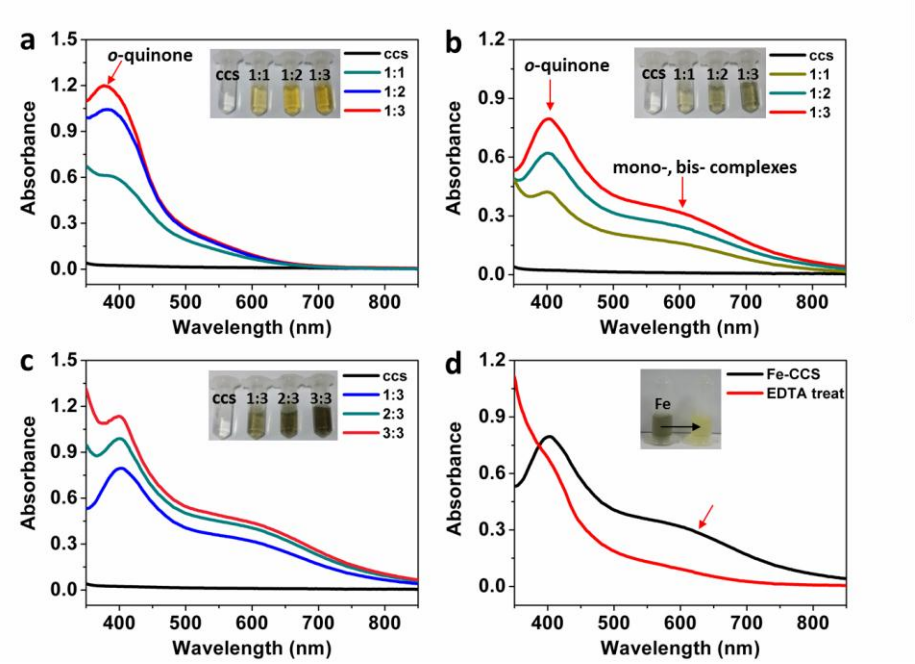

Fig. 5 UV-vis absorbance of Fe^{3+}/IO_4^--CCS in 5% acetic acid solution. (a) Mixed spectra of IO_4^- and CCS (IO_4^--catechol), and (b, c) Fe^{3+} and CCS (Fe^{3+}-catechol). (d) Spectra obtained before and after

EDTA treatment of the Fe^{3+}-CCS solution (Fe^{3+}-catechol ratio of 1:3).

As seen in Fig. 5b, the Fe^{3+}-CCS mixture rapidly yielded a hybrid yellow-green color, which was demonstrated by two strong absorption peaks at ~400 nm, and between ~500 nm and ~700 nm. These results suggest that Fe^{3+} could significantly induce the oxidation of catechol to quinone, as well as coordination with catechols (primarily a mixture of mono- and bis-catechol-Fe^{3+} complexes) in 5% acetic acid.[15] Upon the addition of greater molar quantities of Fe^{3+} (Fig. 5c), a similar absorption spectrum was observed at 400 nm, compared to the spectrum obtained between ~500 nm and ~700nm, but with higher growth. This result indicated that equimolar quantities of Fe^{3+} and catechol could induce greater oxidation; however, this did not significantly contribute to the coordination mechanism because of the increased formation of mono-catechol-Fe^{3+} motifs.

The addition of EDTA to chelate Fe^{3+} caused the yellow-green color to disappear immediately, resulting in a dominantly yellow-colored solution; the peak between ~500nm and ~700 nm was also observed to disappear (Fig. 5d). This revealed that EDTA severed the coordination bond between Fe^{3+} and catechols; only the oxidation residues remained in the solution, caused by the redox activity of Fe^{3+}.

3.5 Resonance Raman spectroscopy

Raman spectroscopy, performed with a visible (514 nm) laser, demonstrated the resonance Raman spectral characteristics of Fe^{3+}-catechol coordination in the hydrogel

network. As seen in Fig. 6, resonance peaks were not observed in the CCS spectra. On the other hand, clear spectral differences were observed between the other samples following the addition of Fe^{3+}, especially in the 500–700 cm^{-1} region that represented the features of Fe-O bond vibrations.[1,15] This region consisted of three major peaks that were transformed clearly according to the variations in the Fe^{3+}-catechol ratios. Specifically, the peak at 531 cm^{-1} indicated the charge transfer (CT) interactions of the bidentate chelate. The hydrogels with a Fe^{3+}-catechol ratio of 1:3 exhibited the highest CT peak intensity, compared to the hydrogels composed of other Fe^{3+}-catechol ratios. The progression of the intensity of CT peaks suggested an increase in the bi-dentate complex formation, which was consistent with the transition from mono- to bis-/tris-catecholate species.[15,23]

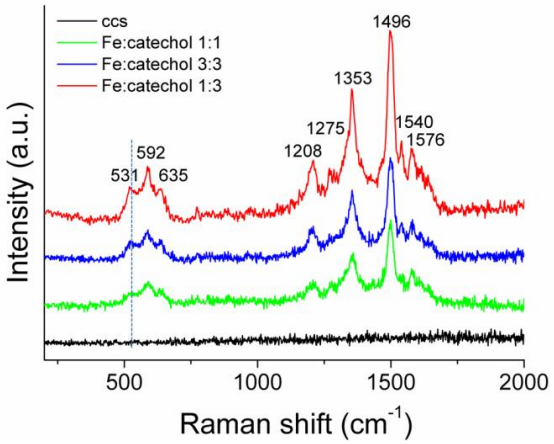

Fig. 6 Resonance Raman spectroscopy of CCS and Fe^{3+}-CCS hydrogels.

3.6 Hydrogel morphology and structure

The morphology of the Fe^{3+}-induced CCS hydrogels before and after EDTA treatment

was observed using an optical microscope, and the results displayed in Fig. 7. The hydrogels generally displayed a smooth, uniform surface with no striations, prior to the EDTA treatment (Fig. 7a). However, an interesting pattern, resembling a spider-web network structure, was observed after EDTA addition (Fig. 7b). These special networks were composed of numerous tiny fibers that adhered and were crosslinked to each other. This morphological change depicted the disintegration of the Fe^{3+}-catechol coordination crosslinking network following EDTA addition; as a result, only the oxidation crosslinking network induced by Fe^{3+} remained in the gel network. In comparison, the optical micrograph of the IO_4^--induced CCS hydrogel (Fig. 7c) revealed a rough non-homogenous, heavily wrinkled surface. CCS is a highly substituted linear polysaccharide; therefore, any exposure to oxidants would easily induce crosslinking among the CCS molecules, thereby forming a thick, string-like structure. However, Fe^{3+}-induced coordination crosslinking is slightly more full-scale. These results visually describe the dual crosslinking structure (coordination and oxidation) of the Fe^{3+}-CCS hydrogel. The hypothetical mechanism has been illustrated in Scheme 1.

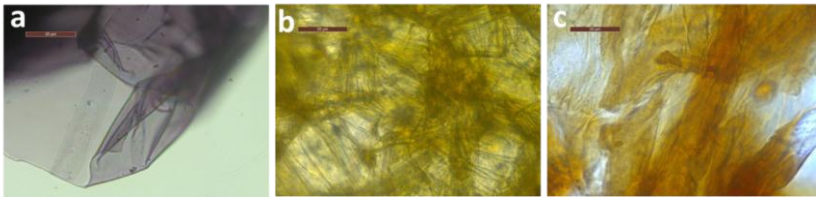

Fig. 7 Optical micrographs of Fe^{3+}-CCS hydrogel (a) before and (b) after EDTA treatment. (c) Optical micrographs of the IO_4^--CCS hydrogel. Scale bars represent 20 μm.

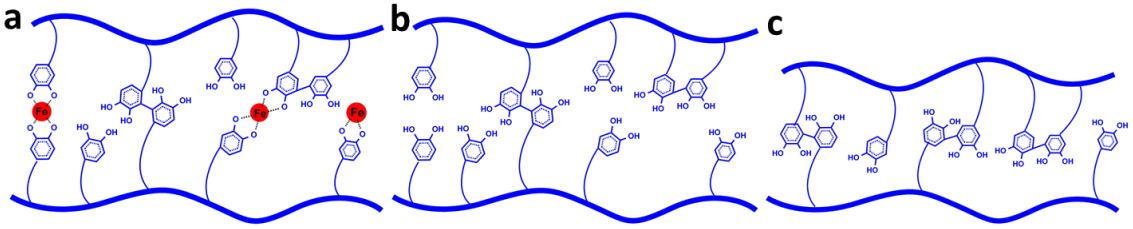

Scheme 1 The plausible mechanism by which crosslinking occurs in the Fe^{3+}-CCS hydrogel (a) before and (b) after EDTA treatment; (c) mechanism of crosslinking in the IO_4^--CCS hydrogel.

The structure of the interiors of these hydrogels was investigated by SEM analysis. As seen in Fig. 8a and 8d, the interior surface of the Fe^{3+}-induced CCS hydrogels was very smooth. This is mainly because the particular structure of catechol-modified chitosan (CCS) and the dual crosslinking mechanism induced by Fe^{3+}. In this work, a long-chain chitosan modified with highly substituted catechol units was used to design Fe^{3+}-CCS hydrogel. With this particular structure, it was easy for CCS to entangle with each other. Furthermore, the addition of Fe^{3+} induced CCS intermolecular crosslinking by forming covalent (quinone-quinone) and coordination bonds (Fe^{3+}-catechol). This leads to a relatively high cross-linking density. However, treatment with EDTA resulted in a lamellar structure with honeycomb-like pores (Fig. 8b, 8e). The 3-dimensional interior morphology of this hydrogel demonstrated a loose, spongy structure, with a large number of internal spaces and irregular linking bridges. On the other hand, the structure of IO_4^--induced CCS hydrogels was relatively flat with rough surfaces (Fig. 8c, 8f). The structural differences among the three CCS hydrogels suggested that the addition of Fe^{3+} to the catechol-chitosan solutions induced oxidation and coordination, resulting in the

formation of different crosslinking structures. This was accompanied with simultaneous interactions among the molecules of the gel structure.

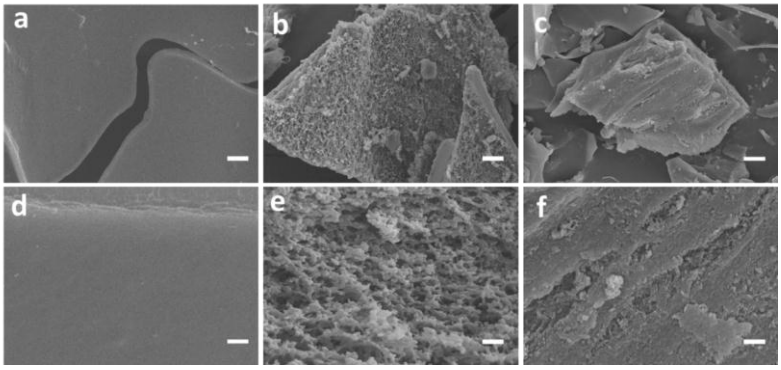

Fig. 8 SEM images of the Fe^{3+}-CCS hydrogel (a, d) before and (b, e) after EDTA treatment; (c, f) SEM images of the IO_4^--CCS hydrogel (scale bars: a, b, c 10 µm; d, e, f 1 µm).

3.7 pH influence on the Fe^{3+}-catechol interactions

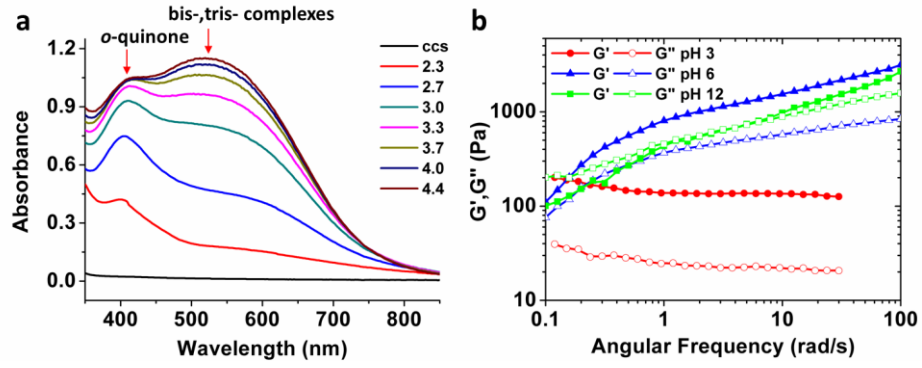

Fig. 9 (a) UV-vis spectra of Fe^{3+}-CCS solution (Fe^{3+}-catechol ratio 1:3) affected by pH increase (effected by titration with 1M NaOH). (b) Frequency sweep of Fe^{3+}-CCS hydrogels (Fe^{3+}-catechol ratio 1:3) adjusted to pH 3, 6, and 12.

All the above analyses were conducted at an acidic pH (pH ~ 3). Therefore, we

attempted to determine the effect of pH on the interactions between Fe^{3+} and catechols. The Fe^{3+}-catechol interactions are known to produce a signature color as a function of pH.[15] In this study, when Fe^{3+} and catechol-chitosan (molar ratio 1:3) were combined at a pH of 2.3, 3.0, and 4.4, the solutions became yellow-green, light purple red, and deep purple red, respectively. In addition, there was a shift in the UV-vis absorption peak to ~450-600 nm (Fig. 9a), which implied the presence of a mixture of bis- and tris-catechol-Fe^{3+} complexes within the solution. Generally, bis- and tris-catecholate motifs formation is believed to occur at neutral and alkaline pH, respectively.[15] These results may have been obtained as a result of the particular structure of CCS (linear, high substitution degree of catechol), which facilitates the formation of bis- and tris-catechol-Fe^{3+} complexes even under acidic pH conditions. With the increase of pH, the absorption peak at ~500-800nm (coordination region) experienced a higher growth than the one at ~400nm (oxidation region). This result confirmed that the rise in pH positively affected the Fe^{3+}-catechol coordination, but negatively affected catechol oxidation.[15,18]

In addition, we attempted to elucidate the impact of pH on the mechanical properties of Fe^{3+}-CCS hydrogels (Fig. 9b). Fe^{3+} and catechol-chitosan were combined at pH 3, 6, and 12; this resulted in a drastic change in the color and physical properties from a dark gel to a red clumpy material. The rheological properties are listed in Fig. 9b. The increase in pH gradually imparted a Maxwell-like behavior to the Fe^{3+}-CCS hydrogel, indicated

by the clear crossover in the frequency sweep at pH 12. This change in behavior indicated that the dual-crosslinking system (pH 3) is converted to a coordination-dominated system (pH 12), possibly in a tris-catecholate configuration.[15,18]

4. Conclusions

A natural, linear copolymer modified with highly substituted catechol units was used to design a novel, biologically inspired hydrogel in this study. A dual-crosslinking system composed of covalent and coordination interactions was observed at acidic pH. SEM and optical micrograph analyses were used to visually describe this crosslinking network. In addition, this dual crosslinking system was fortified with a greater number of coordination bonds upon regulation of the pH of the Fe^{3+}-catechol-modified chitosan reaction. The results of this study indicated that the chemical structure of the hydrogel, in addition to the pH, composition, and processing method, is required to mimic the mussel byssal threads, highlighting the opportunities related to the design of novel mussel-inspired materials. Reasonable manipulation of these variables would afford access to a broad spectrum of physical properties reflecting the balance between covalent and coordination crosslinking in the hydrogel network.

Author information

Corresponding Authors

*E-mail: yhren@ecust.edu.cn

Notes

The authors declare no competing financial interest.

Acknowledgements

This work was funded by the National Special Fund for the State Key Laboratory of Bioreactor Engineering (2060204), the National Natural Science Foundation of China (No. 21076079), the National major science and technology projects of China (No. 2012ZX09304009), and the Fundamental Research Funds for the Central Universities of China.

References

(1) M. J. Harrington, A. Masic, N. Holten-Andersen, J. H. Waite, P. Fratzl, Iron-clad fibers: a metal-based biological strategy for hard flexible coatings, *Science*, 2010, **328**, 216-220.

(2) J. H. Waite, Evidence for a repeating 3,4-dihydroxyphenylalanine- and hydroxyproline-containing decapeptide in the adhesive protein of the Mussel, mytilus edulis L, *J. Biol. Chem*., 1983, **258**, 2911-2915.

(3) S. W. Taylor, G. W. Luther, J. H. Waite, Polarographic and spectrophotometric investigation of iron(III) complexation to 3,4-dihydroxyphenylalanine-containing peptides and proteins from mytilus edulis, *Inorg. Chem*., 1994, **33**, 5819-5824.

(4) J. H. Waite, M. L. Tanzer, Polyphenolic substance of mytilus edulis: novel adhesive containing L-dopa and hydroxyproline, *Science*, 1981, **212**, 1038-1040.

(5) J. H. Waite, Nature's underwater adhesive specialist, *Int. J. Adhes. Adhes*., 1987, **7**, 9-14.

(6) E. Vaccaro, J. H. Waite, Yield and post-yield behavior of mussel byssal thread: a self-healing biomolecular material, *Biomacromolecules,* 2001, **2**, 906-911.

(7) H. Zhao, J. H. Waite, Proteins in load-bearing junctions: the histidine-rich metal-binding protein of mussel byssus, *Biochemistry,* 2006, **45**, 14223-14231.

(8) M. J. Harrington, J. H. Waite, Holdfast heroics: comparing the molecular and mechanical properties of mytilus californianus byssal threads, *J. Exp. Biol*, 2007, **210**, 4307-4318.

(9) B. P. Lee, P. B. Messersmith, J. N. Israelachvili, J. H. Waite, Mussel-inspired adhesives and coatings, *Annu. Rev. Mater. Res*., 2011, **41**, 99-132.

(10) M. J. Harrington, J. H. Waite, pH-dependent locking of giant mesogens in fibers drawn from mussel byssal collagens, *Biomacromolecules,* 2008, **9**, 1480-1486.

(11) H. Zeng, D. S. Hwang, J. N. Israelachvili, J. H. Waite, Strong reversible Fe^{3+}-mediated bridging between dopa-containing protein films in water, *Proc. Natl. Acad. Sci. U.S.A.*, 2010, **107**, 12850-12853.

(12) J. J. Wilker, The iron-fortified adhesive system of marine mussels, Angew. Chem. Int. Ed., 2010, **49**, 8076 – 8078.

(13) M. Krogsgaard, M. A. Behrens, J. S. Pedersen, H. Birkedal, Self-healing mussel-inspired multi-pH-responsive hydrogels, *Biomacromolecules,* 2013, **14**, 297-301.

(14) C. E. Brubaker, H. Kissler, L. J. Wang, D. B. Kaufman, P. B. Messersmith, Biological performance of mussel-inspired adhesive in extrahepatic islet transplantation, *Biomaterials*, 2010, **31**, 420-427.

(15) N. Holten-Andersen, M. J. Harrington, H. Birkedal, B. P. Lee, P. B. Messersmith, K. Y. C. Lee, J. H. Waite, pH-induced metal-ligand cross-links inspired by mussel yield self-healing polymer networks with near-covalent elastic moduli, *Proc. Natl. Acad. Sci. U.S.A.*, 2011, **108**, 2651-2655.

(16) E. Mentasi, E. Pelizzetti, Reactions between iron(III) and catechol (o-dihydroxybenzene). part I. equilibria and kinetics of complex formation in aqueous acid solution, *J. Chem. Soc., Dalton Trans*., 1973, **23**, 2605-2608.

(17) E. Mentasi, E. Pelizzetti, G. Saini, Reactions between iron(III) and catechol (o-dihydroxybenzene). part II. equilibria and kinetics of the redox reaction in aqueous acid solution, *J. Chem. Soc., Dalton Trans*., 1973, **23**, 2609-2614.

(18) D. G. Barrett, D. E. Fullenkamp, L. He, N. Holten-Andersen, K. Y. C. Lee, P. B. Messersmith, pH-based regulation of hydrogel mechanical properties through mussel-inspired chemistry and processing, *Adv. Funct. Mater*., 2013, **23**, 1111-1119.

(19) D. E. Fullenkamp, D. G. Barrett, D. R. Miller, J. W. Kurutz, P. B. Messersmith, pH-dependent cross-linking of catechols through oxidation via Fe^{3+} and potential implications for mussel adhesion, *RSC Adv*., 2014, **4**, 25127-25134.

(20) B. P. Lee, J. L. Dalsin, P. B. Messersmith, Synthesis and gelation of dopa-modified poly(ethylene glycol) hydrogels, *Biomacromolecules*, 2001, **3**, 1038-1047.

(21) J. Desbrieres, C. Martinez, M. Rinaudo, Hydrophobic derivatives of chitosan: characterization and rheological behaviour, *Int. J. Biol. Macromol*., 1996, **19**, 21-28.

(22) C. E. Orrego, N. Salgado, J. S. Valencia, G. I. Giraldo, O. H. Giraldo, C. A. Cardona, Novel chitosan membranes as support for lipases immobilization: characterization aspects, *Carbohydr. Polym*., 2010, **79**, 9-16.

(23) S. W. Taylor, D. B. Chase, M. H. Emptage, M. J. Nelson, J. H. Waite, Ferric ion complexes of a dopa-containing adhesive protein from mytilus edulis, *Inorg. Chem*., 1996, **35**, 7572–7577.

Table of Contents

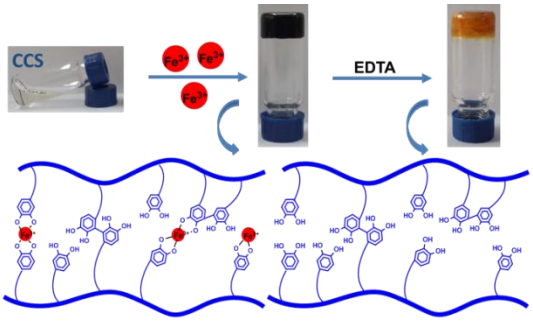

Fe^{3+}-induced oxidation and coordination cross-linking in catechol-chitosan (CCS) hydrogels under acidic pH conditions; When this Fe^{3+}-CCS hydrogel was exposed to EDTA, the coordination crosslinking system was disrupted, but the covalently-crosslinked residues remained untouched.